Journal of Thermal Analysis and Calorimetry, Vol. 85 (2006) 2, 315–320

THERMAL BEHAVIOR OF AMMONIUM PERCHLORATE AND METAL POWDERS OF DIFFERENT GRADES

J. Zhi[1], *W. Tian-Fang*[1], *L. Shu-Fen*[1*], *Z. Feng-Qi*[2], *L. Zi-Ru*[2], *Y. Cui-Mei*[2], *L. Yang*[2], *L. Shang-Wen*[2] *and Z. Gang-Zhui*[3]

[1]Department of Chemistry Physics, University of Science and Technology of China, Hefei 230026, P.R. China
[2]Xian Modern Chemistry Research Institute, Xian 710065, P.R. China
[3]Shanxi Institute of Power Machinery, Xian 710025, P.R. China

The effects of aluminum (Al) and nickel (Ni) powders of various grain sizes on the thermal decomposition of ammonium perchlorate (AP) were investigated by TG and DSC in a dynamic nitrogen atmosphere. The TG results show that Al powders have no effect on the thermal decomposition of AP at conventional grain size, while the nanometer-sized Ni powders (n-Ni) have a great influence on the thermal decomposition of AP with conventional and superfine grain size. The results obtained by DSC and an in situ FTIR analysis of the solid residues confirmed the promoting effects of n-Ni. The effects of n-Ni have been ascribed to its enhancement on the gas phase reactions during the second step decomposition of conventional grain size AP.

Keywords: *aluminum, ammonium perchlorate, FTIR, nano metal powder, nickel*

Introduction

Great interest has been generated by the development of nano materials. Nano materials are represented by particles with average grain diameters in the range of 1 to 100 nm [1–2]. One interesting characteristic of nano powders is that the number of atoms at the surface of the particle is comparable with the number of atoms in the bulk of the particle. Nano materials also contain lattices with high concentrations of dislocations and large surface areas. Thus, nano materials exhibit high chemical reactivity, which allows a number of nanometer-sized metals to undergo reactions that were previously considered impossible. New types of propellant containing nano metal powder have been developed [3–6].

AP is one of the main oxidizing agents used in various propellants. The burning behavior of propellants is sensitive to the thermal decomposition of oxidizing agents like AP. Understanding of the complex physicochemical processes that underlying the thermal decomposition of such materials can provide a link between the thermal decomposition and the burning process of the propellant. Many investigators have studied the thermal decomposition of AP as a neat compound or as mixtures in the presence of certain inorganic materials, such as metals, metal oxides and other salts [7–20]. However, the AP investigated were only of coarse grain size (g-AP) [7–14, 16–18, 20]. Little research has been extended on AP of fine grain size. Because AP of different grain size will have different thermal behavior, studies extended on superfine AP (s-AP) or nanometer-sized AP will lead to interesting results [19]. Furthermore, most of the researches carried out on investigating the thermal behavior of AP were only based on TG and DTA [7–14]. Such studies may lead to a rather speculative mechanism with no further supporting evidence. Further studies should be carried out based on the thermal analysis together with some other techniques. FTIR techniques have been widely used today to characterize materials [21, 22]. In particular, in situ FTIR analysis, which can follow sample residue's FTIR properties over a long period of time at a specified temperature, is a technique which provides data for a comprehensive understanding decomposition processes.

In the present work, the effects of Al and Ni powders of different grain sizes on the thermal decomposition characteristics of g-AP have been studied by TG. As the TG results show that n-Ni have a great influence on the thermal decomposition of g-AP. The studies are specifically extended to investigate the decomposition of g-AP and the g-AP and n-Ni mixture by DSC and in-situ FTIR. The thermal decomposition of s-AP and the s-AP/n-Ni and s-AP/s-Ni mixture have also been studied by TG. Such studies may offer useful clues for the application of nano metal powders in propellants in order to obtain a better control of their combustion.

Experimental

Samples

The powdered sample of AP (technical pure) was sieved to two grain diameters (g-AP, 80 μm; s-AP 1.1 μm).

* Author for correspondence: lsf@ustc.edu.cn

1388–6150/$20.00

Akadémiai Kiadó, Budapest, Hungary
Springer, Dordrecht, The Netherlands

Mixtures of metal powders and g-AP were prepared by carefully mixing of the two components in a polished porcelain container with acetone as the dispersant. The g-AP and metal powders mixtures with mass ratio of 4:1, 8:1 and 16:1 are prepared. Mixtures of metal powders and s-AP were prepared by mechanical mixing only in the absence of the dispersant. The s-AP and n-Ni mixtures with mass ratio of 4:1 are prepared. The metal powders used in this study were: g-Al (10 μm, supplied by Xian Modern Chemistry Research Inst.), nano aluminum (n-Al, 83 nm, produced by the electro-explosion process, oxygen content <1.8mass%, supplied by Sheng Tai nano Ltd.), superfine nickel powders (s-Ni, 3 μm, supplied by Xian Modern Chemistry Research Inst.) and n-Ni (16 nm, prepared by γ-ray radiation synthesis method in our laboratory). The procedures of the preparation of n-Ni are described in the next section. The grain size of the samples is specified by the manufacturer.

The solutions for γ-ray radiation were prepared by dissolving analytically neat $NiSO_4 \cdot 6H_2O$ in distilled water. $NH_3 \cdot H_2O$ was added as a complexing agent for Ni^{2+} ions and NH_3H_2O/NH_4^+ buffer pair to adjust the pH of the solution. Sodium dodecyl sulphate was used as a surfactant, and isopropanol was used as a scavenger for hydroxyl radicals in our experiments. The solutions were de-aerated by bubbling with neat nitrogen, and then irradiated in the field of a $2.59 \cdot 10^{15}$ Bq ^{60}Co γ-ray source. After irradiation, the metal particles were separated from solutions, washed with distilled water several times, and then dried to powders in vacuum. All reagents used in the radiation experiment above were analytically pure grade. The Ni powders were then collected in hexane (commercial quality) to prevent the oxidation of n-Ni powders in air [23]. The grain size of n-Ni was determined using a D/Max-rA X-ray diffractometer (CuK_α radiation), Rigaku. The calculated results show that the average grain size of the n-Ni is 16 nm.

Instrumental

The thermal decomposition analysis was performed by using a differential scanning calorimeter, (TA Instruments, DSC Model 910), and a thermogravimetric analyzer (TA Instruments, TA Model 2950). A constant sample mass of 2.0±0.1 mg was used in all experiments. TG and DSC were performed in a dynamic atmosphere of nitrogen with flow rates of 100 and 40 mL min^{-1}, respectively. The TG and DSC experiments were performed using open platinum sample pans and sealed Al sample pans, respectively. In this paper, the enthalpy values for the g-AP and n-Ni mixture are based on per gram of g-AP, but not the mixture. The in-situ FTIR spectra of g-AP and the g-AP/n-Ni mixture were recorded with a Nicolet MAGNA-IR 750 spectrometer using KBr pellets in the temperature range of 20–420°C with an interval of 10°C and a heating rate of 2°C min^{-1} in air atmospheres. The FTIR analysis was performed on the solid residue of the sample during the thermal decomposition.

Results and discussion

TG and DSC for the mixtures of AP and metal powders

The TG/DTG data for g-AP and the mixtures of g-AP and metal powders (with mass ratio of 4:1) are summarized in Table 1. The TG/DTG curves for g-AP in nitrogen show two mass loss steps (Fig. 1). The first step is accompanied by about 25% mass loss in the temperature range of 280 to 329°C (i.e., the low-temperature decomposition step). The second step is accompanied by about 72% mass loss in the temperature range of 329 to 370°C (i.e., the high-temperature decomposition step). Addition of Al powders (n-Al and g-Al) only slightly lowers the peak temperature of the high-temperature decomposition of g-AP and has almost no effect on the low-temperature decomposition of g-AP (Table 1). While for the mixture of g-AP and n-Ni, the second step of the decomposition of g-AP was notably enhanced by the addition of n-Ni pow-

Table 1 TG/DTG data for AP and mixture of AP/metal powders

Sample	T_p/°C	
	LTD	HTD
g-AP	307	353
g-AP/n-Ni	312	327
g-AP/s-Ni	309	330
g-AP/n-Al	308	348
g-AP/g-Al	311	350

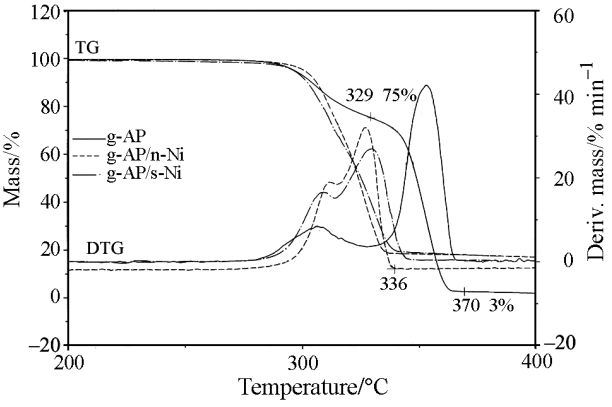

Fig. 1 TG/DTG curves for g-AP, g-AP/s-Ni(4:1) and g-AP/n-Ni (4:1) in nitrogen (0.1 MPa; 10°C min^{-1})

ders, since the g-AP/n-Ni mixture displayed a large DTG peak at 327°C and was completed at 336°C (Fig. 1). The advance of the second step causes more overlapping between the two steps of decomposition of g-AP into nearly one step. Compared to s-Ni, the presence of n-Ni shifted the end temperature and the DTG peak for the second step of g-AP decomposition to a lower temperature. The results suggest that n-Ni is more effective than s-Ni on promoting the decomposition of g-AP.

The DSC curve for g-AP is shown in Fig. 2. The DSC data for g-AP and the g-AP and metal powders mixture (with mass ratio of 4:1) are summarized in Table 2.

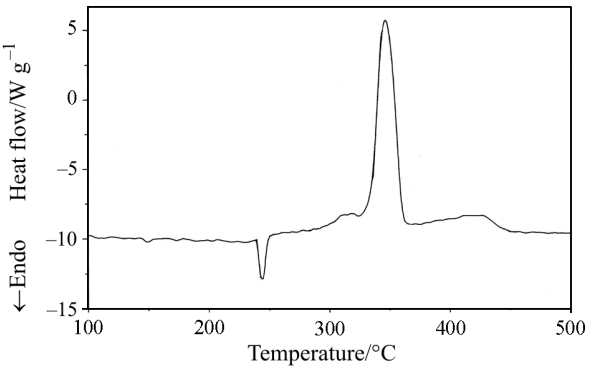

Fig. 2 DSC curve for g-AP in nitrogen (0.1 MPa; 10°C min^{-1})

The weak endothermic with peak temperature 244°C on the DSC curves for g-AP is due to the crystal transformation of AP from orthorhombic to cubic. Two main exothermic peaks remain around 318 and 347°C, respectively. They correspond to the two mass loss steps on the TG/DTG curves for g-AP (Fig. 1). As shown in Fig. 1, the decomposition of g-AP is clearly a two-step process. However, three exothermic peaks are observed in the DSC (Fig. 2). The third exothermic peak for neat AP is observed from 370°C to above 450°C (Fig. 2). As the TG/DTG curves for g-AP (Fig. 1) has shown that 2.6% residues will remain when the whole decomposition has completed at 370°C. An inconspicuous mass loss process will exist above 370°C. And because the TG experiments were performed using open pans, while the DSC with closed containers. Secondary reactions take place between the gases trapped in the closed pan will notably enhance the reactions above 370°C. All these will lead to the third exothermic peak for neat AP observed from 370°C to above 450°C. With the addition of n-Ni, the weak endotherm of g-AP phase transition remains around 244°C, the first and third exothermic peak is absent. And the thermal decomposition of the g-AP/n-Ni mixture shows only one overlapping exotherm peaked at 322°C and ended at 350°C. The third exothermic peak for neat g-AP above 370°C is not observed for the g-AP/n-Ni mixture. The overlapped exotherm is consistent with the TG/DTG data illustrated in Fig. 1.

The TG/DTG curves for the mixtures of g-AP and n-Ni with mass ratios of 4:1, 8:1 and 16:1 are shown in Fig. 3. The TG/DTG data are summarized in Table 3. The DTG peak temperature for the mixtures increases gradually with a decrease of n-Ni content. When the mass ratio of g-AP to n-Ni is changed from 4:1 to 16:1, the first-step peak temperature of g-AP changes from 312 to 308°C. In the second step, the peak temperature decreases 18.0 from 353°C for neat g-AP to 335°C for the g-AP/n-Ni (16:1) mixture. It is interesting that the peak temperature in the low-temperature decomposition step of g-AP is higher when metals are added (Figs 1 and 2). With the decrease of the content of n-Ni, the peak temperatures for the low-temperature decomposition step of g-AP will decrease simultaneously (Fig. 3). The previous DSC studies (Table 2) also showed that the total heat released during the decomposition step of neat g-AP is lower from 2177 to 1330 J g^{-1} when n-Ni powders are added. The decrease in the heat released together with increasing peak temperature for the low-temperature

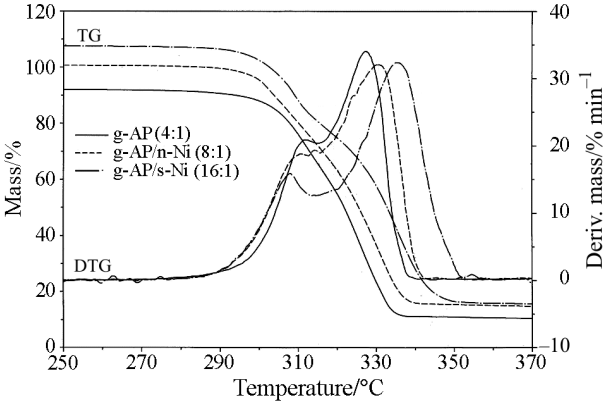

Fig. 3 TG/DTG curves for g-AP with various n-Ni contents in nitrogen (0.1 MPa; 10°C min^{-1})

Table 2 DSC data of g-AP and mixture of g-AP/n-Ni metal powders

Sample	T_s/°C	LTD		HTD			Third stage	
		T_p/°C	ΔH/J g^{-1}	T_p/°C	T_e/°C	ΔH/J g^{-1}	T_p/°C	ΔH/J g^{-1}
g-AP	245	318	180	347	370	1619	426	378
g-AP/n-Ni	244			322	450	1330		

decomposition step of g-AP when 20 mass% of n-Ni is added may be due that the metal is inert in the first step and acts as a heat sink.

The decomposition of g-AP is clearly a two-step process. For s-AP, there is only one DTG peak at 357°C corresponding to the high-temperature step decomposition as shown in Fig. 4. The TG/DTG data for s-AP and the s-AP and n-Ni mixture (with mass ratio of 4:1) are summarized in Table 3.

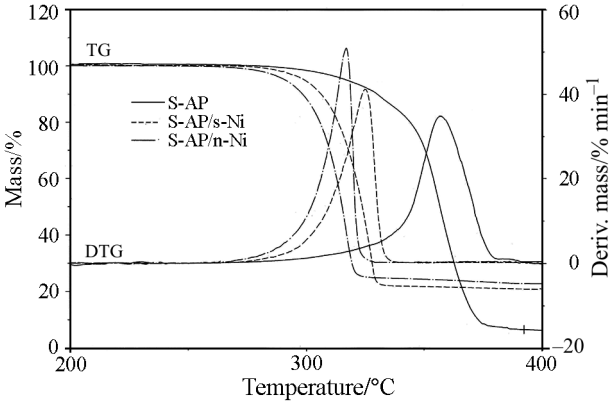

Fig. 4 TG/DTG curves for s-AP, s-AP/n-Ni (4:1) and s-AP/s-Ni (4:1) in nitrogen (0.1 MPa; 10°C min^{-1})

Table 3 TG/DTG data for g-AP and mixture of g-AP and n-Ni with different content

Sample	T_p/°C	
	LTD	HTD
g-AP/n-Ni (4:1)	312	327
g-AP/n-Ni (8:1)	311	330
g-AP/n-Ni (16:1)	308	335

It is considered that the thermal decomposition of solid AP occurs at some partial surface sites of its crystal. For large crystal grain size (i.e. g-AP), the reaction site (nucleus formation) forms easily on the crystal surface and the reaction rate increases [13]. That makes the large crystal cracks and forms smaller crystals. If NH_3 (gas) released during the decomposition of AP overspread the whole active center, the decomposition of AP begins the slow process. When temperature rise continuously, the potential reaction centers will be activated again by the desorption of NH_3. For s-AP, the internal stress formed by decomposition products is not intensive enough to crack the AP crystal into smaller grains. So, there is none exist of distinctly low temperature decomposition step because NH_3 formed in the initial steps overspread the crystal surface of s-AP. Thus the thermal decomposition of s-AP provided an opportunity to evaluate the high-temperature step decomposition of g-AP.

The addition of n-Ni lowers the peak temperature of s-AP by 40°C, which is similar to the promoting effects of n-Ni on the high temperature decomposition step of g-AP. The addition of s-Ni to s-AP also lowers the DTG peak temperature of s-AP by 32°C. Thus, compared to s-Ni, n-Ni is more effective in promoting the decomposition of s-AP.

In-situ FTIR analysis for g-AP and the mixtures of g-AP and n-Ni

The FTIR results presented in this paper are some examples of our first effort to study the thermal decomposition of AP. In-situ FTIR was used to compare the solid residues obtained from the thermal decomposition of neat g-AP and the g-AP/n-Ni mixture.

The FTIR spectra at 20°C for g-AP and the g-AP/n-Ni mixture are shown in Fig. 5. The peaks at 3300–3000 and 1409 cm^{-1} (1571–1245 cm^{-1}) can be assigned to the stretching and bending vibrations of the N–H bond in the NH_4^+ ion, and the peaks at around 1088 and 627 cm^{-1} can be assigned to the ClO_4^- anion

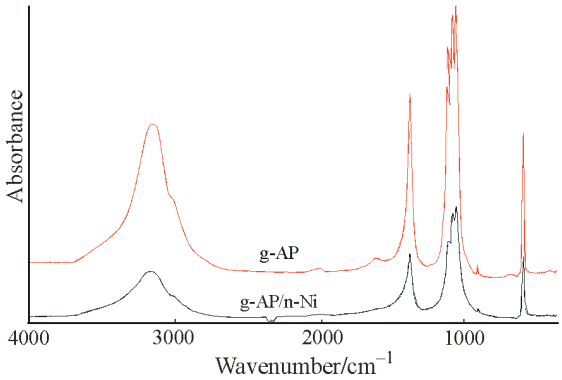

Fig. 5 FTIR spectra for g-AP and g-AP/n-Ni at 20°C in air

[24].

The FTIR spectra for g-AP at the low-temperature range (200, 280 and 310°C) and high-temperature range (360 and 400°C) are compared to that for 20°C in Fig. 6. The intensities of the peaks at 3300–3000 and 1409 cm^{-1} (N–H) decrease as the temperature increases. The spectra obtained for 400°C show that the intensities are about 10 and 5% of those for 20°C. And they remained as weak peaks when the temperature was raised to 400°C. The intensity of the peaks at around 1088 and 627 cm^{-1} decreased slowly between 200 and 400°C. When the temperature reached 400°C, the peak area around 1088 and 627 cm^{-1} has decreased nearly to half of that value at 20°C.

The relatively slower disappearance of ClO_4^- in the lattice may be due to the electron-transfer during the thermal decomposition of AP. Electron-transfer in the AP crystal will lead to the conversion of NH_4ClO_4

into NH_4+ClO_4, followed by the dissociation of NH_4 to NH_3+H, and the transfer of charge between ClO_4 and ClO_4^- within the lattice until a free ClO_4 reaches the surface of the particle [8, 12–14]. At the surface of the particle, it undergoes decomposition to gaseous products. This means that the disappearance of ClO_4^- will lag behind the disappearance of NH_4^+ in the crystal lattice, which corresponds with the FTIR results shown in Fig. 6.

The FTIR spectra for g-AP/n-Ni at the temperatures 20, 200, 280 and 310°C shown in Fig. 7 are similar to that of g-AP shown in Fig. 6. That is, in the temperature range of 200–310°C, the n-Ni powders have no promoting effect in the low temperature decomposition step of g-AP. These provide direct evidence to support the conclusion drawn from the thermal analysis experiment, i.e., the metal is inert in the first step and acts as a heat sink.

The difference for g-AP/n-Ni and g-AP lies in the FTIR spectra under heating conditions 360 and 400°C, as shown in Fig. 7. The addition of n-Ni to g-AP leads to a rapid decrease of the intensity of peaks related to the vibration of N–H at 3300–3000 and 1409 cm^{-1}. They had nearly completely disappeared when the temperature reached 400°C. While the intensities of the peaks at around 1088 and 627 cm^{-1} decreased quickly between 200 and 400°C as compared with the slower process relating to the decomposition of neat g-AP shown in Fig. 6. When the temperature reached 400°C, the peaks for g-AP/n-Ni at around 1088 and 627 cm^{-1} showed a weak peak.

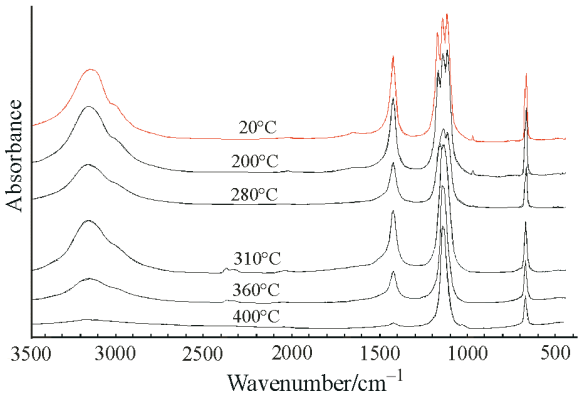

Fig. 6 FTIR spectra for g-AP in air

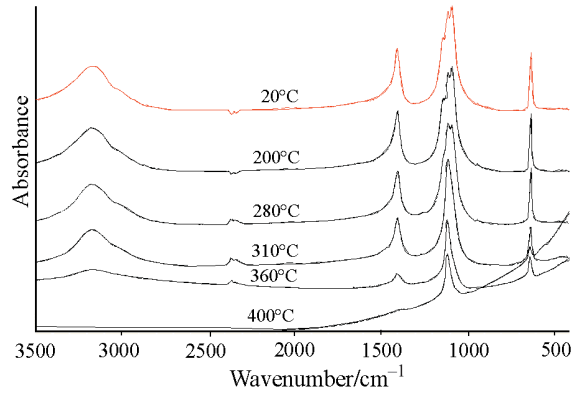

Fig. 7 FTIR spectra for g-AP/n-Ni in air

All these confirm the promoting effects of n-Ni on the second step decomposition of g-AP. It is known that the decomposition of neat AP is controlled by two processes. One occurs at lower temperature (240 to 270°C) and produces mainly H_2O, O_2, Cl_2, N_2O, NH_3 and HCl, and is shown to occur in the solid phase within the AP crystal. The second process is dissociative sublimation of AP to NH_3+$HClO_4$ followed by reactions between these two products in the gas phase [7, 15]. Thus the promoting effects of n-Ni on the second step may be ascribed to promote the gas phase reactions during the decomposition of g-AP.

As previous studies have revealed, in the presence of the transition metal or transition metal oxides, the gaseous oxygen-rich products, such as $HClO_4$ (g), may migrate to the surface of the transition metal or transition metal oxides by surface diffusion and decompose heterogeneously [12, 16]. n-Ni will be able to greatly promote the redox reactions between the given gaseous products, especially those released from ClO_4^-, which are oxidative rich. The quick decrease of the intensity of the peak related to ClO_4^- in g-AP with the existence of n-Ni (Fig. 7) has provide evidence to support such inference. During the step of high temperature decomposition of AP, the gas-phase reactions will then be influenced. It will lead to a change in the distribution of the gaseous products. The decomposition of g-AP is then promoted.

Conclusions

The effects of aluminum and nickel powders of various grain sizes on the thermal decomposition of AP were investigated by TG and DSC in a dynamic nitrogen atmosphere. The thermal decomposition of g-AP showed two separate mass-loss steps. The TG results show that aluminum powders have no effect on the thermal decomposition of AP, while the n-Ni powders have a great influence on the thermal decomposition of g-AP and s-AP. The results show that n-Ni mainly promote the second step decomposition of g-AP, while it is inert in the first step and acts as a heat sink. The results of the in-situ FTIR for the decomposition residue of g-AP confirmed the promoting effects of n-Ni. The dominant effects of n-Ni may be ascribed to promotion of the gas phase reactions during the second step of the decomposition of g-AP. That is to promote the redox reaction rate between the gaseous products during the thermal decomposition of AP. The FTIR results also suggest that the disappearance

of ClO_4^- will lag behind the disappearance of NH_4^+ in the crystal lattice during the heating conditions, which provides evidence to support the proposed speculative electron-transfer mechanism.

Acknowledgements

We greatly appreciate the financial support provided by the National Natural Science Foundation of China (No. 50476025).

Nomenclature

Al	aluminum
AP	ammonium perchlorate
DSC	differential scanning calorimeter
DTA	differential thermal analysis
DTG	derivative thermogravimetry
FTIR	Fourier transform infrared spectroscopy
g-Al	micron-sized Al powder (10 μm)
g-AP	conventional AP powder (80 μm)
HTD	step of high temperature decomposition
LTD	step of low temperature decomposition
n-Al	nanometer-sized Al powder (83 nm)
Ni	nickel
n-Ni	nanometer-sized Ni powder (16 nm)
s-AP	superfine AP (1.1 μm)
s-Ni	superfine nickel powders (3 μm)
TG	thermogravimetry
T_p	peak temperature of DTG and DSC
T_s	crystal transformation temperature of AP from orthorhombic to cubic
T_e	end temperature of decomposition

References

1 A. Henglein, Chem. Rev., 89 (1989) 1861.
2 R. E. Caviechi and R. H. Silsbee, Phys. Rev. Lett., 52 (1984) 1453.
3 G. V. Ivanov and F. Tepper, Challenges in Propellants and Combustion 100 Years after Nobel, Begell House, New York 1997, p. 636.
4 Z. Jiang, S. F Li and F. Q. Zhao, J. Energ. Mater., 20 (2002) 165.
5 D. A. Yagodnikov and A. V. Voronetskii, Combust. Expl. Shock, 33 (1997) 49.
6 M. M. Mench, K. K. Kuo, C. L.Yeh and Y. C. Lu, Combust. Sci. Technol., 135 (1998) 269.
7 K. K. Kuo and M. Summerfield, Fundamental of Solid Propellant Combustion, AIAA. Inc., New York 1984, p. 53.
8 A. A. Said, J. Thermal Anal., 37 (1991) 959.
9 A. A. Said and R. AlQasmi, Thermochim. Acta, 275 (1996) 83.
10 S. A. Halawy and S. S. Al-Shihry, J. Therm. Anal. Cal., 55 (1999) 833.
11 S. A. Halawy and M.A. Mohamed, Collect. Czech. Chem. Commun., 59 (1994) 2253.
12 L. L. Liu, F. S. Li, L. H. Tan, Propellants, Explos., Pyrotech., 29 (2004) 34.
13 P. W. M. Jacobs, Combus. Flame, 13 (1969) 419.
14 T. Ganga Devi, M. P. Kannan and B. Hema, Thermochim. Acta, 285 (1996) 269.
15 L. Rosso and M. E. Pure, Appl. Chem., 76 (2004) 49.
16 R. Behrens and L.Minier, Sand-97-8422C.
17 K. Kishore and M. R. Sunitha, AIAA Journal, 17 (1979) 1118.
18 M. Rajic and M. Suceska, J. Therm. Anal. Cal., 63 (2001) 375.
19 A. Pivkina, Yu. Frolov, S. Zavyalov, 31st International Pyrotechnics Seminar, Fort Collins, CO, July 11–16, 2004, p. 285.
20 J. A. F. Rocco, J. E. S. Lima and A. G. Frutuoso, J. Therm. Anal. Cal., 77 (2004) 803.
21 M. F. Silva, C. A. da Silva and F. C. Fogo, J. Therm. Anal. Cal., 79 (2004) 367.
22 F. Barontini, K. Marsanich and V. Cozzani, J. Therm. Anal. Cal., 78 (2004) 599.
23 Y. Champion and J. Bigot, Nanostr. Mat., 10 (1998) 1097.
24 G. Socrates, Infrared and Raman characteristic group frequencies: tables and charts, Chichester, England: Wiley, 2001.

Received: July 11, 2005
Accepted: July 27, 2005
OnlineFirst: December 12, 2005

DOI: 10.1007/s10973-005-7035-7